JOURNAL OF GEOPHYSICAL RESEARCH, VOL. 100, NO. D7, PAGES 13,967–13,978, JULY 20, 1995

Interhemispheric differences in springtime production of HCl and $ClONO_2$ in the polar vortices

Anne R. Douglass,[1] Mark R. Schoeberl,[1] Richard S. Stolarski,[1] J. W. Waters,[2] James M. Russell III,[3] Aidan E. Roche,[4] Steven T. Massie [5]

Abstract. UARS observations of O_3 and ClO (Microwave Limb Sounder), $ClONO_2$ and HNO_3 (Cryogenic Array Etalon Spectrometer), NO, NO_2, and HCl (Halogen Occultation Experiment), and model calculations are used to produce an exposition of the different processes through which the reservoir gases $ClONO_2$ and HCl are reformed at the end of the polar winter. Comparison of the observations within the polar vortices shows that HCl increases more rapidly in the Antarctic vortex in spring than in the Arctic vortex. Model analysis shows that this occurs because the O_3 concentrations in the southern vortex fall well below those in the northern vortex. The Cl/ClO fraction calculated for the southern hemisphere is therefore up to 30 times higher, leading to rapid HCl formation by Cl + CH_4 . The concentrations of NO observed by HALOE are substantially lower for the northern hemisphere than for the southern hemisphere, even for similar values of the concentration of HNO_3 and the production of NO_X from HNO_3 through photolysis and reaction with OH. This is consistent with the dependence of the NO/NO_X ratio on the O_3 concentration, i.e., the daytime production rate of NO_2 via NO + O_3 is reduced, leading to higher NO in the southern hemisphere. This higher concentration of NO also contributes to the rapid HCl increase as Cl production from ClO + NO is enhanced.

Introduction

The processes which lead to polar ozone depletion have been fairly well established through observations and modeling, as was discussed in a review article by *Solomon* [1990]. As a result of heterogeneous reactions of the chlorine reservoir species $ClONO_2$ and HCl on polar stratospheric clouds, ClO and the dimer Cl_2O_2 become the dominant chlorine species [e.g., *Solomon et al.*, 1986; *Anderson et al.*, 1989; *de Zafra et al.*, 1989]. The catalytic destruction of O_3 occurs with the formation of the dimer Cl_2O_2; subsequent photolysis of the dimer, producing two Cl atoms; and reaction of Cl with O_3 to reform ClO [*Molina and Molina*, 1987]. The concentration of ClO is observed to remain high until vortex temperatures rise above polar stratospheric cloud (PSC) formation temperatures [*Waters et al.*, 1993; *Toohey et al.*, 1993; *Schoeberl et al.*, 1993].

It has long been known that the hemispheres differ in that the temperatures within the northern vortex are substantially warmer than those in the southern vortex [e.g., *Schumacher*, 1955]; *Randel* [1992] provides a recent statistical comparison of the northern and southern hemispheres. The temperature difference is large enough that PSC formation is different in the two hemispheres. The formation threshold for nitric acid trihydrate clouds (type I) is about 195 K at 50 hPa for 10 ppbv HNO_3 and 5 ppmv H_2O. The formation temperature for ice clouds (type II) is about 7 K colder. In the northern vortex, temperatures are seldom cold enough to support type II cloud formation. When the temperatures rise above the type I condensation temperature, the HNO_3 is returned to the gas phase. Subsequently, formation of $ClONO_2$ following production of NO_X through photolysis of HNO_3 and reaction of HNO_3 with OH competes effectively with chlorine-catalyzed ozone destruction. Elevated levels of $ClONO_2$ have been observed within the northern vortex [*Mankin et al.*, 1990]. Large O_3 loss is not observed. *Prather and Jaffe* [1990] show that for ozone concentrations and odd nitrogen concentrations typical of the northern vortex, the equilibrium between the chlorine reservoirs is reestablished slowly because of the slow rate of Cl + CH_4 .

Deep within the southern vortex, the temperatures are cold enough that formation of type II PSCs is possible. In situ data suggest the permanent removal from

[1]NASA Goddard Space Flight Center, Greenbelt, Maryland.
[2]Jet Propulsion Laboratory, California Institute of Technology, Pasadena, California.
[3]NASA Langley Research Center, Hampton, Virginia.
[4]Lockheed Palo Alto Research Laboratory, Palo Alto, California.
[5]National Center for Atmospheric Research, Boulder, Colorado.

Paper number 95JD00698.
0148-0227/95/95JD-00698$05.00

the lower stratosphere of both H_2O (dehydration) and HNO_3 (denitrification)[*Fahey et al.*, 1990]; satellite observations show the spatial and temporal dependencies of these processes [e.g.,*McCormick et al.*, 1989; *Roche et al.*, 1993a]. In the springtime, chlorine catalized destruction of O_3 proceeds in denitrified air without interference from nitrogen radicals via $ClONO_2$ formation. When the O_3 concentration reaches extremely low values, the production of ClO from the reaction of Cl with O_3 slows, the concentration of Cl rises, and production of HCl by $Cl + CH_4$ takes place rapidly [*Prather and Jaffe*, 1990].

The purpose of this paper is to use UARS observations to examine the reformation of chlorine reservoir species within the Arctic polar vortex and in the region just inside the southern vortex boundary. In this "collar" region, which is warmer than the vortex core, HNO_3 concentrations measured by the Cryogenic Array Etalon Spectrometer (CLAES) during austral spring are similar to those observed throughout the springtime in the northern vortex. UARS data provide information on the key species involved in chemical processes occurring within these two regions. The Microwave Limb Sounder (MLS, version 3) measures O_3 and ClO [*Barath et al.*, 1993]. There are two radiometer channels on MLS which measure O_3; this paper will use data from the 205 GHz radiometer channel. The CLAES (version 7) measures O_3, $ClONO_2$, and HNO_3 [*Roche et al.*, 1993b], and the Halogen Occultation Experiment (HALOE, version 17) measures HCl, O_3, NO, and NO_2 [*Russell et al.*, 1993]. For all UARS instruments, the version number associated with the instrument refers to the retrieval algorithm used to produce the data set. MLS and CLAES are limb-sounding instruments that provide near coincident measurements. HALOE observations are made at sunrise and sunset. The latitudes at which UARS sees sunrise and sunset change each day, and HALOE observes the polar regions during different periods than do the other instruments. In order to organize the data for comparison, the data, which are reported for each instrument for standard pressure levels, are interpolated onto potential temperature surfaces and averaged with respect to potential vorticity [*Schoeberl et al.*, 1989; *Manney et al.*, 1994; *Schoeberl et al.*, 1995]. The differences in the production of chlorine reservoir species HCl and $ClONO_2$ within the southern hemisphere collar compared with that observed within the northern hemisphere vortex will be emphasized here.

Observations

Southern hemisphere maps of $ClONO_2$ and HNO_3 measured by CLAES and ClO and O_3 measured by MLS for September 17, 1992, are shown in Plate 1. Contours of potential vorticity are shown in white, and the nominal vortex edge is between the two outermost contours (-2 and -3 $\times$ 10^{-5} K $m^2kg^{-1}s^{-1}$). For both $ClONO_2$ and HNO_3, a mixing ratio maximum appears poleward of the vortex edge. The high values of $ClONO_2$ are colocated with high concentrations of HNO_3. Both HNO_3 and $ClONO_2$ decrease poleward of this "collar" region. High daytime ClO concentrations are seen by MLS in the region of low HNO_3 and $ClONO_2$.

The northern hemisphere maps of $ClONO_2$, HNO_3, ClO, and O_3 for March 2, 1992, are shown in Plate 2. The contours of potential vorticity are shown in white. In contrast to the southern hemisphere, the vortex ClO values are barely elevated above the threshold for detection by an individual MLS measurement (0.4 ppbv). The O_3 concentrations are much higher than those within the southern vortex. The concentrations of HNO_3 and $ClONO_2$ are somewhat larger than southern collar values and are nearly uniform throughout the vortex.

Because of the strong shear, mixing tends to be more rapid along contours of potential vorticity than across the contours. This is apparent from the distribution of long-lived species which tend to be highly correlated with potential vorticity [*Schoeberl and Lait*, 1992, and references therein]. Reactive species do not exhibit this high correlation with potential vorticity. However, because parcel trajectories tend to follow potential vorticity contours, parcels with the same potential vorticity are assumed to have similar experience with respect to temperature, solar insolation, and time in polar stratospheric clouds. For this study we use modified potential vorticity (MPV), a form of potential vorticity that has conservation properties similar to those of Ertel's potential vorticity but without the exponential variation with height [*Lait*, 1994].

The UARS data for each constituent are averaged in bins defined by values of MPV. For a distorted polar vortex, the average concentration within an MPV bin will be substantially different from a zonal average concentration. As was mentioned above, CLAES and MLS observe high southern latitudes until late September, when the spacecraft is yawed to north viewing. HALOE observes sunrises and sunsets at a different latitude each day and views high southern latitudes during late September and October. For the austral collar region, the data are averaged within the band MPV=$(-4.0 \pm 0.2) \times 10^{-5}$ K $m^2kg^{-1}s^{-1}$ indicated by black and yellow contours in Plate 1. Time series for August 1 - November 1, 1992, are given at potential temperature 460 K for O_3, $ClONO_2$, HNO_3, HCl, NO, NO_2, H_2O, temperature, and average latitude of observations within each MPV band in Plate 3. The vertical bars indicate the standard deviation for the observations. For the northern hemisphere, data are averaged within the band MPV=$(3.0 \pm 0.2) \times 10^{-5}$ K $m^2kg^{-1}s^{-1}$ shown by black and yellow contours in Plate 2. Time series of the constituents, temperature, and average latitude of observations at potential temperature 480 K are shown for February 1 - May 1 in Plate 4. A time series for daytime ClO is also given in both figures. Observations from a wider MPV bin are used in the ClO average. A slightly higher potential temperature is used in the north, since the vortex is warmer. The average

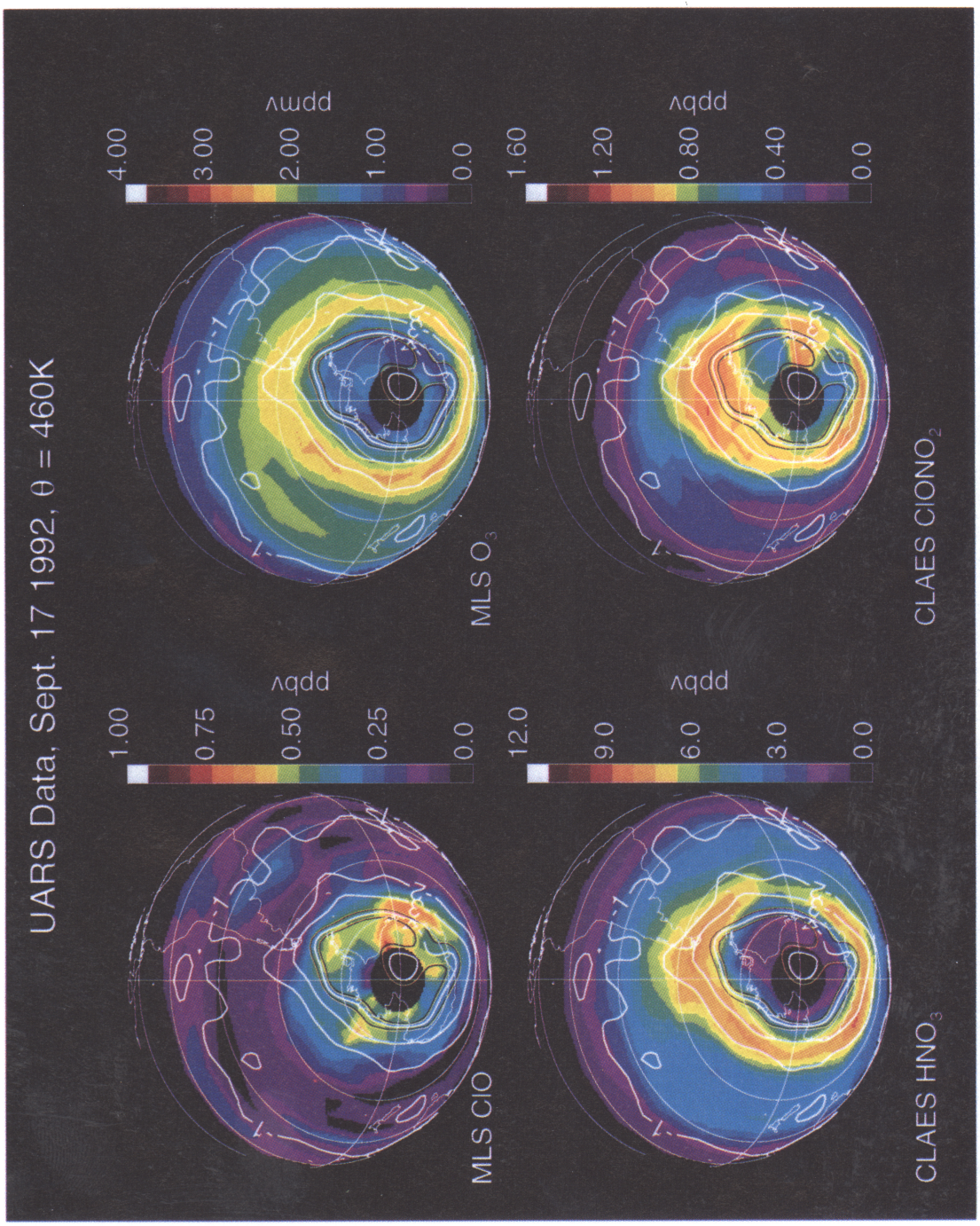

Plate 1. UARS observations of ClO, O_3, $ClONO_2$, and HNO_3 for the southern hemisphere in September 1992. The white solid lines are MPV contours. The observations within the tube banded by thin yellow and black lines are considered here.

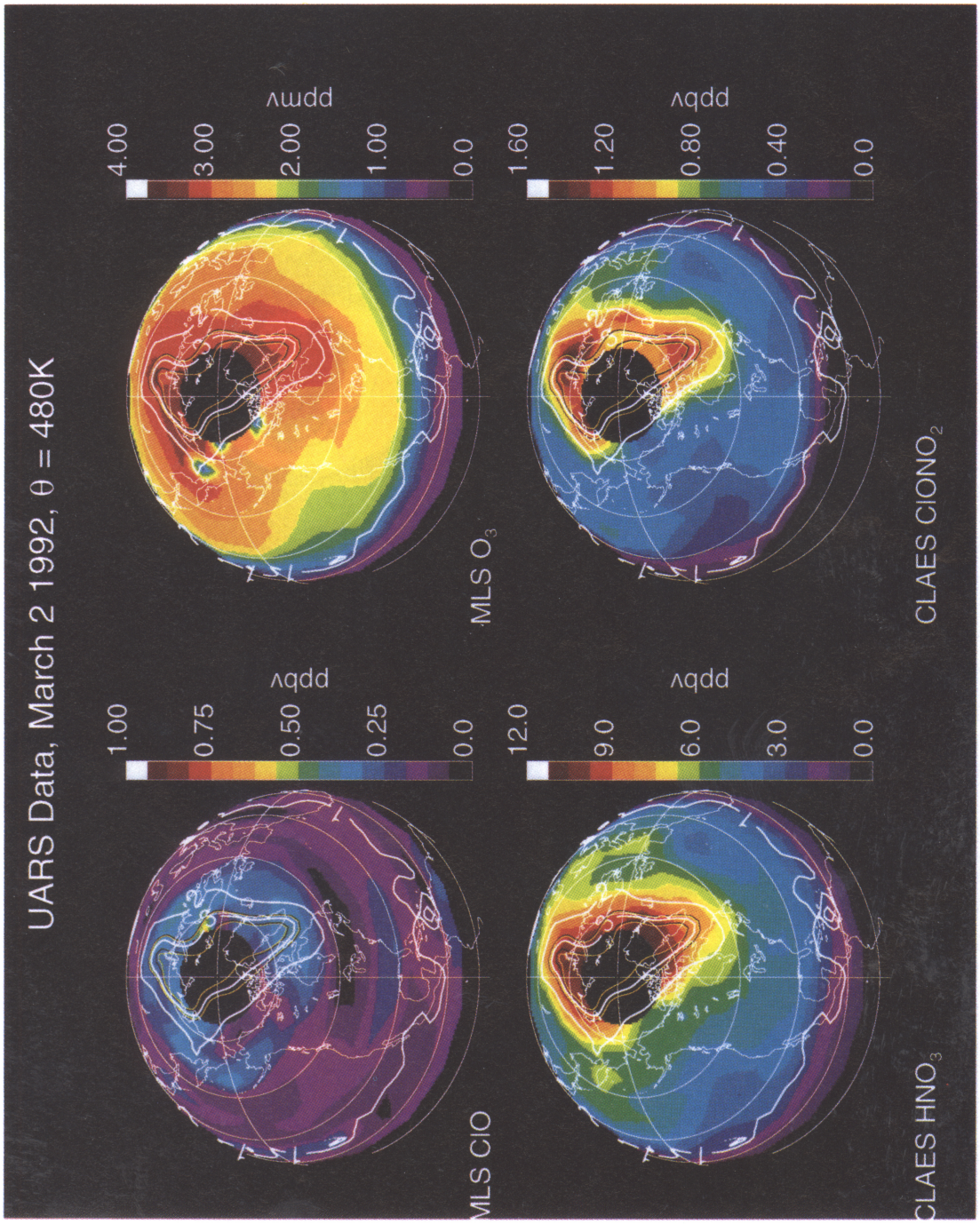

Plate 2. UARS observations of ClO, O_3, $ClONO_2$, and HNO_3 for the northern hemisphere in March 1992. The white solid lines are MPV contours. The observations within the tube banded by thin yellow and black lines are considered here.

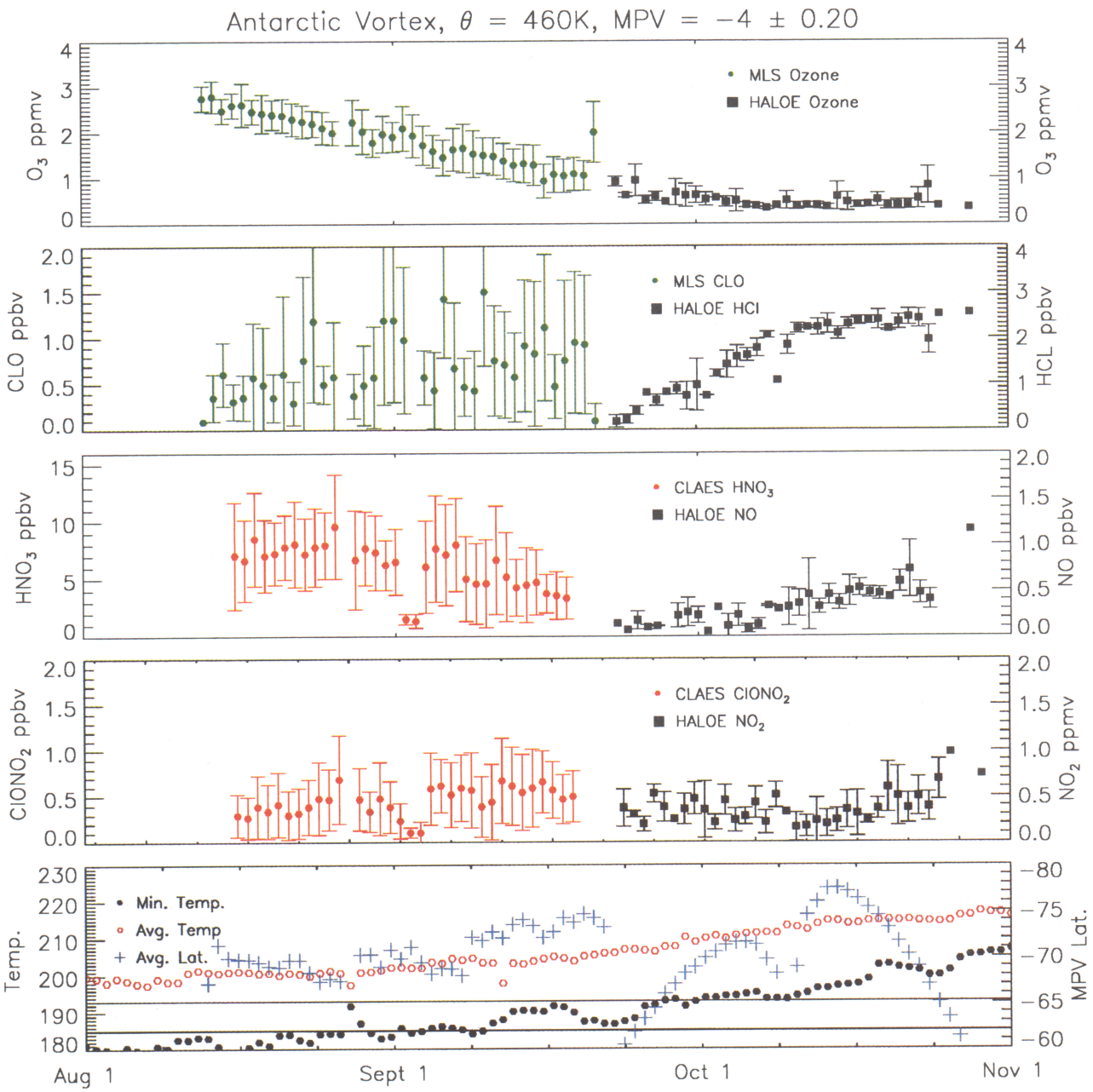

Plate 3. Time series of southern hemisphere observations binned by MPV.

latitudes of these MPV contours are similar; the times of the year are identical with respect to the winter solstice.

In the southern hemisphere spring, the ozone concentration decreases steadily. Even though the average latitude of HALOE observations at this MPV value is farther from the pole than the average latitude of MLS observations, there is no discontinuity in the O_3 time series. The daytime average ClO values are between 0.5 and 1 ppbv. HCl and NO grow substantially during October, from near zero at the beginning of October to more than 2 ppbv for HCl and about 0.5 ppbv for NO at the end of October. NO_2 is somewhat larger at the end of October than at the beginning but has not increased steadily. HNO_3 and $ClONO_2$ are nearly constant through most of September. HNO_3 decreases somewhat toward the end of the yaw cycle.

In the northern hemisphere, MLS and HALOE O_3 observations do not agree with each other during late March, when there are measurements from both instruments within the MPV bin. However, the HALOE observations are within the standard deviation of the MLS observations. The difference between MLS and HALOE ozone values is explained by the location of the 480 K potential temperature surface relative to the pressure levels at which MLS retrieves ozone mixing ratios. For temperatures warmer than 199 K, typical of this time period in the northern hemisphere (Plate 4), the 480 K potential temperature surface is at a higher pressure (lower altitude) than the MLS retrieval level at 46 hPa.

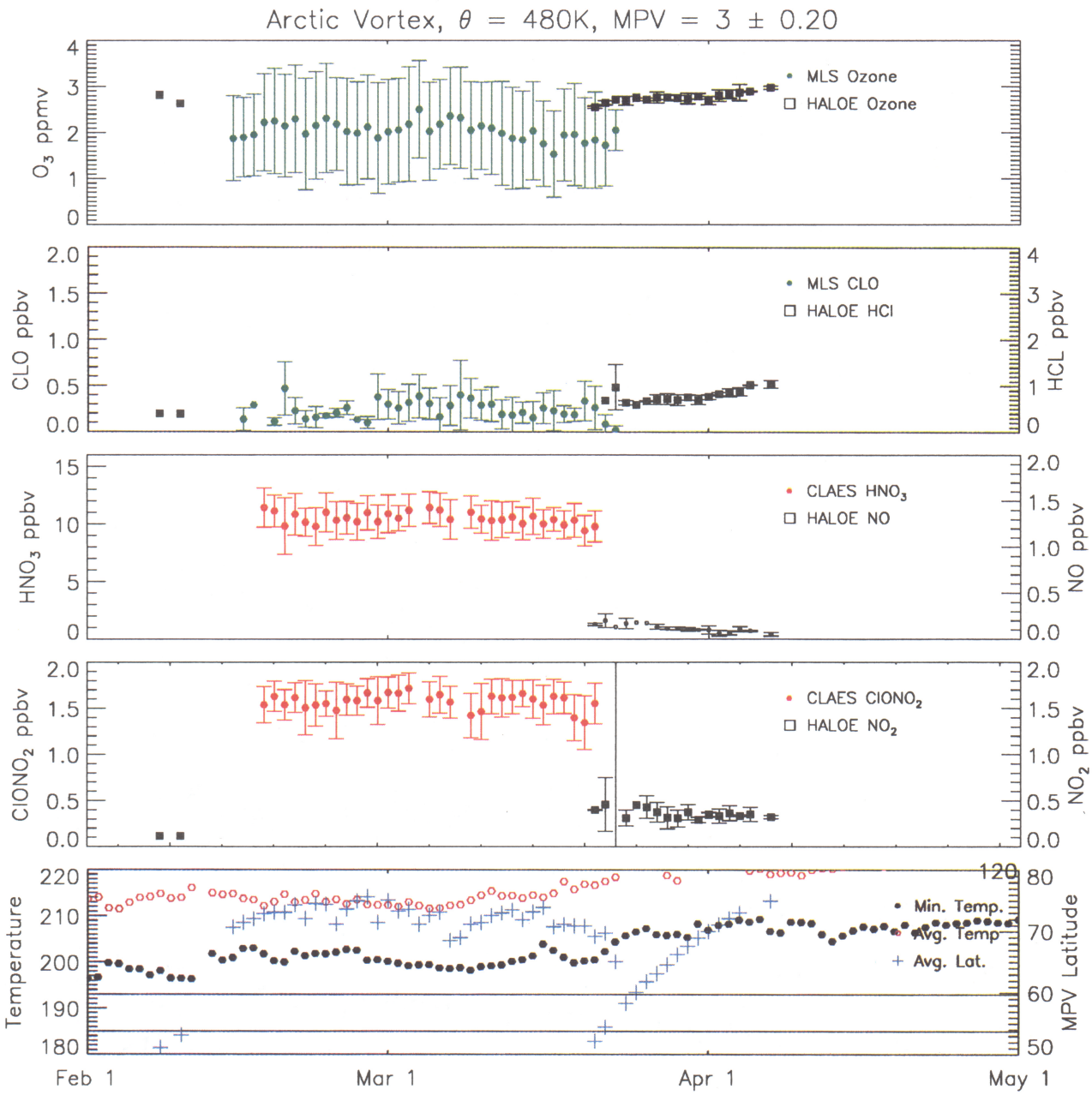

Plate 4. Time series of northern hemisphere observations binned by MPV.

The precision and accuracy of the MLS ozone for the 205 GHz radiometer channel are estimated to be 0.2 ppmv and 30% at 46 hPa, and 0.5 ppmv and $\geq$ 50% at 100 hPa. The HALOE observations have higher vertical resolution, equal to about 2 km with an estimated precision and accuracy of 0.2 ppmv and 18% at 40 hPa and 0.1 ppmv and 30% at 100 hPa. Thus the shape of the ozone mixing ratio profile between 46 hPa and 100 hPa is not determined as well by MLS as by HALOE. The MLS ozone mixing ratios at higher potential temperature (e.g., 520 K) are between the 46-hPa and 21.5-hPa pressure surfaces. The precision and accuracy in the MLS ozone mixing ratio at 21.5 hPa are about 0.2 ppmv and 7%, and interpolated values are in better agreement with HALOE data.

Fortunately, the systematic difference at 480 K between the HALOE and MLS average values is not important to this discussion. The important observations which should be contrasted with the southern hemisphere situation are that neither instrument shows very low ($\leq$ 1 ppmv) average O_3 values and neither instrument suggests an O_3 trend. The daytime ClO concentrations in the northern hemisphere are smaller than those in the southern hemisphere throughout the period. HALOE HCl observations near the beginning of the UARS northward viewing yaw cycle are a few tenths of a part per billion by volume. During the few weeks following the northward viewing cycle, HCl gradually increases. CLAES $ClONO_2$ concentrations are close to 2 ppbv, substantially larger than the southern hemi-

sphere value, and exhibit no clear trend. HALOE NO concentrations, highest at the beginning of October, are very low throughout the period. NO_2 concentrations are larger than these NO concentrations and suggest no trend. HNO_3 concentrations are larger than those in the southern hemisphere (about 10 ppbv compared with 7 ppbv) and are steady.

Model Calculations

The chemical changes expected during the time period of the observations are calculated using a box model. This model has previously been used with a trajectory model to show that a substantial component of the variance in aircraft ClO observations is explained by the differing amounts of insolation received by parcels along the flight track since their last encounter with cold temperatures [*Schoeberl et al.*, 1993]. The chemical model includes O_3, NO_y, HO_x, Cl_y, and Br_y species. Diurnal changes are resolved by using a time step of 180 s. Photolysis rates are calculated using cross section data from *DeMore et al.* [1992], with the exception of the HNO_3 temperature dependent cross sections, which are taken from *Burkholder et al.* [1993]. Radiative transfer including multiple scattering is calculated using a look-up table; the computations are based on the work of *Anderson and Lloyd* [1990]. Reaction rates are calculated using data from *DeMore et al.* [1992]. For heterogeneous reactions on aerosol surfaces $ClONO_2 + H_2O$ and $N_2O_5 + H_2O$, reaction rates are calculated as is recommended in chapter 8 of World Meteorological Organization (1992):

$$\text{rate} = 5200 \text{ cm s}^{-1} \times G \times SA \quad (1)$$

where 5200 cm s^{-1} is an effective collision velocity, G is the probability of reaction per collision, and SA is the surface area density. For $N_2O_5 + H_2O$,$G = 0.1$. For $ClONO_2 + H_2O$, $G = 0.006 \times \exp(-0.15 \times (T - 200))$where $T$is the temperature; this formula is a fit to laboratory data of *Tolbert et al.* [1988] for stratospheric conditions. Reactions on PSCs are not included explicitly. The initial conditions for each hemisphere assume that PSC reactions have already taken place. The HCl concentration is so low during the time that the temperatures are cold enough to support PSC formation that further reactions on PSCs involving HCl would have little or no effect. At temperatures cold enough for PSC formation, the reaction of $ClONO_2 + H_2O$ proceeds on aerosol surfaces at a rate comparable to that on PSC surfaces. These reactions are not distinguishable in the model. The calculations in this paper are intended to be illustrative and are used to identify the processes which explain the observed behavior. They are not intended to replicate the observations quantitatively.

Calculations are shown for each hemisphere. The parcel location each day is the average of the latitudes for the observations within the MPV band. The parcel temperature is the average temperature for the MPV band. The model initialization is based on the observations. The initial ozone is 2.5 ppmv in each case. For the southern hemisphere calculations, inorganic chlorine is 3.4 ppbv; HCl is initially zero, and $ClONO_2$ is 0.4 ppbv; the remainder of inorganic chlorine is ClO or Cl_2O_2. The reactive nitrogen is assumed to be zero, as is suggested by the very low HALOE NO observations in late September and also as is expected from the high values of ClO; HNO_3 is initially 7 ppbv. In the northern hemisphere, HCl and $ClONO_2$ are 10% and 60% of the initial Cl_y, as is suggested by the HALOE and CLAES data. The model results may be sensitive to the rate of the reaction $ClONO_2 + H_2O$, particularly in the southern hemisphere because the temperatures are colder. Calculations are shown for two values of aerosol surface area: the median value for the last 2 decades 2.5×10^{-8}cm^{2}cm^{-3} [*WMO*, 1992], and 4 times this value. These calculations demonstrate the sensitivity of the results to surface area, which is probably elevated as a result of the 1991 eruption of Mount Pinatubo.

Model time series for the MPV=$(-4.0 \pm 0.2) \times 10^{-5}$ K m^{2}kg^{-1}s^{-1} are shown in Figure 1. Many but not all of the features seen in the observations are duplicated by these calculations. The trend in O_3 is well reproduced: rapid loss in September is followed by a leveling off at a low value in October. A calculated decrease in HNO_3 due to photolysis and reaction with OH is similar to that suggested by the data. The steep rise in HCl throughout October is accompanied by a substantial increase in NO. In the model, NO_2 increases along with NO; this increase is not seen in the data. The calculated increase for $ClONO_2$ during late August and September is not observed. The modeled increase in $ClONO_2$ and HCl is balanced by the decrease in ClO and twice Cl_2O_2. A decrease in HOCl from the beginning of September through the end of the calculation accounts for less than 10% of the increase in the sum of $ClONO_2$ + HCl.

The model also reproduces much of the behavior seen in the northern hemisphere (Figure 2). In keeping with the low concentration of ClO, only small changes in O_3 are calculated. There is an increase in HCl, but it is not nearly as rapid as that observed or calculated for HCl in the southern hemisphere. The calculated NO is low throughout April despite the significant loss of HNO_3 and the low values of ClO. As in HALOE observations, the concentration of NO_2 is substantially higher than the concentration of NO. In the model, sunrise or sunset NO_2 rises rapidly at the end of April, but NO remains low throughout the period.

The concentrations of ClO and $ClONO_2$ are sensitive to the aerosol surface area. The $ClONO_2$ concentration is smaller for larger surface area, and the ClO concentration is correspondingly higher. In the northern hemisphere, NO and NO_2 concentrations are slightly larger for smaller surface area. In the southern hemisphere, both the NO_x and the fraction NO/NO_x respond indirectly to the change in surface area. Here, in the case of high aerosol surface, O_3 falls to very low values due to loss from enhanced ClO. NO_x increases as $ClONO_2$ is

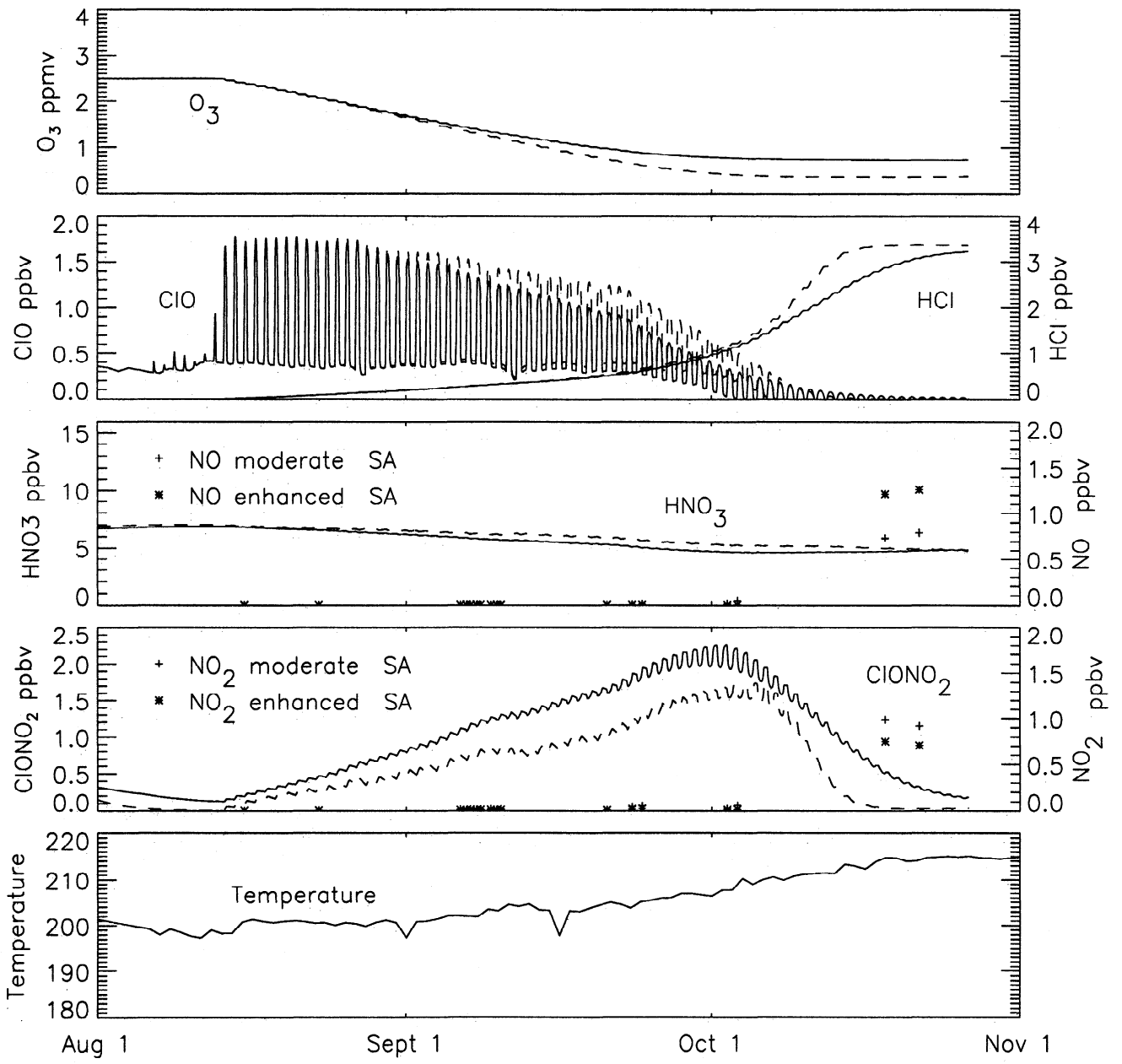

Figure 1. Model calculations are shown for the same time period as the southern hemisphere observations. The solid line is for baseline aerosol surface area; the dashed line is for 4 times that surface area.

converted to HCl, and the NO/NO_X fraction increases due to low O_3 as discussed in the next section.

Discussion

The reduction of the concentration of the radical ClO to a value appropriate for the lower stratosphere in the absence of polar stratospheric clouds takes place through the formation of the reservoir gases $ClONO_2$ and HCl. The formation of $ClONO_2$, through the reaction $ClO+NO_2+M \rightarrow ClONO_2+M$, depends on the concentrations of ClO and NO_2. Since the daytime concentration of ClO is high, the concentration of $ClONO_2$ is limited by the available NO_2. In the absence of near-total denitrification ($HNO_3 \geq \sim 3$ ppbv), $ClONO_2$ formation takes place rapidly as HNO_3 is photolyzed. The formation of HCl is principally through the reaction $Cl+CH_4 \rightarrow HCl+CH_3$. Since the CH_4 mixing ratio is nearly constant throughout the lower stratosphere, the formation rate for HCl is controlled by the concentration of Cl. The reactions through which Cl and ClO are produced and destroyed are rapid; thus the photochemical equilibrium ratio may be derived from the principal production and loss processes:

$$\frac{[Cl]}{[ClO]} = \{k_{ClO,NO}[NO] + 2 \times J_{Cl_2O_2}\frac{[Cl_2O_2]}{[ClO]} + J_{ClONO_2}\frac{[ClONO_2]}{[ClO]} + J_{HOCl}\frac{[HOCl]}{[ClO]}\} \times \{k_{Cl,O_3}[O_3]\}^{-1} \quad (2)$$

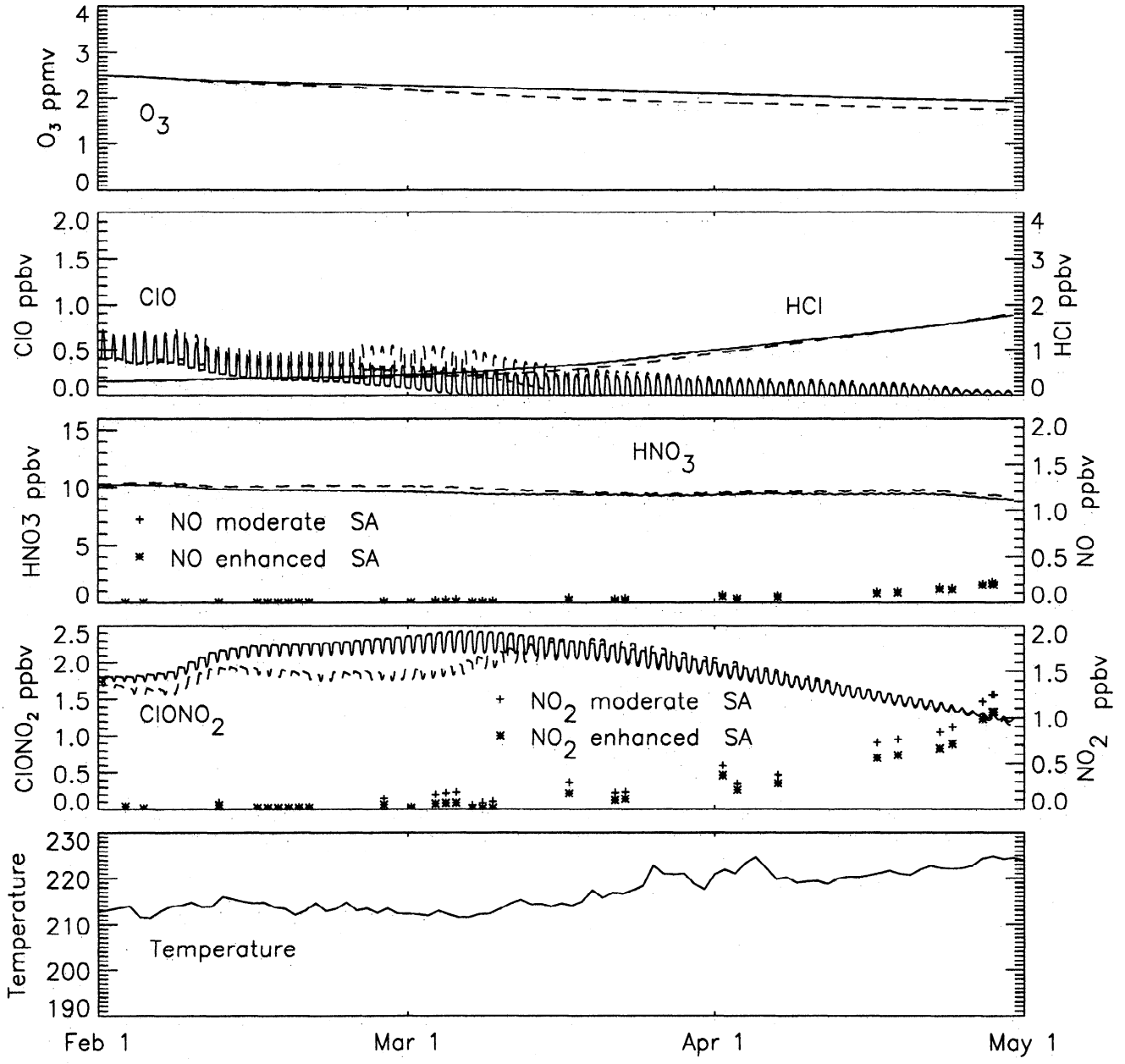

Figure 2. Model calculations are shown for the same time period as the northern hemisphere observations. The solid line is for baseline aerosol surface area; the dashed line is for 4 times that surface area.

Production of Cl via ClO + O is negligible in the lower stratosphere spring. As was noted by *Prather and Jaffe* [1990], for very low NO concentrations and very low O_3 values found deep within the denitrified southern vortex, reaction of ClO with NO and photolysis of $ClONO_2$ can be neglected. The fraction Cl/(Cl + ClO + $2Cl_2O_2$) is enhanced because Cl is produced by photolysis of Cl_2O_2 and the production of ClO via $Cl + O_3 \rightarrow ClO + O_2$ decreases as the O_3 concentration decreases. When denitrification is not so drastic, as in the northern hemisphere or in the southern hemisphere "collar" the reaction ClO+NO dominates the production of Cl once loss of HNO_3 through photolysis and reaction with OH to produce NO_X is significant, even for daytime values of NO as small as 50 ppt. In the model, Cl production through ClO + NO dominates all other pathways beginning in early October in the southern hemisphere. Neglecting photolysis of Cl_2O_2, HOCl and $ClONO_2$, the Cl concentration is proportional to NO, as was suggested by *Liu et al.* [1992], and is also inversely proportional to O_3.

The ratio NO/NO_2 can also be written assuming photochemical equilibrium between principal production and loss processes:

$$\frac{[NO]}{[NO_2]} = \frac{J_{NO_2}}{k_{NO,O_3}[O_3] + k_{ClO,NO}[ClO]} \quad (3)$$

Solving for NO and neglecting the $J_{Cl_2O_2}$, J_{HOCl}, and J_{ClONO_2} terms, the Cl/ClO ratio may be written

$$\frac{[Cl]}{[ClO]} = \frac{J_{NO_2} k_{ClO,NO}[NO_2]}{k_{NO,O_3} k_{Cl,O_3}[O_3]^2 + k_{Cl,O_3} k_{ClO,NO}[O_3][ClO]} \quad (4)$$

For elevated values of ClO, $k_{Cl,O_3} k_{ClO,NO}[O_3][ClO] \gg k_{NO,O_3} k_{Cl,O_3}[O_3]^2$. For normal concentrations of ClO and O_3 the reverse is true, and reactions of NO and Cl with O_3 control the production of ClO. For low O_3 and normal ClO, the two terms may be of similar magnitude; the Cl/ClO ratio increases as O_3 decreases (assuming that ClO is constant or decreasing). HCl production becomes rapid, reaching a maximum of nearly 0.25 ppbv d^{-1}. This is similar to results reported by *Prather and Jaffe* [1990] for air which has been strongly denitrified. For those calculations, $NO_X/NO_y \simeq 0.50$, in contrast to the case here where HNO_3 remains the dominant NO_y species. The NO/NO_2 ratio also responds to ozone behavior. For very low O_3 and low ClO calculated for the southern hemisphere in late October, the daytime ratio NO/NO_2 (equation (2)) is nearly 10 times that calculated for the northern hemisphere in April with low ClO and a higher concentration of O_3. Note that even for the low O_3 and ClO concentrations considered here, the conversion of NO to NO_2 is rapid enough for the use of the photostationary steady state of NO and NO_2. The photolysis rate for HNO_3 is similar in the two calculations. The smaller cross section in the colder southern hemisphere is compensated by a smaller ozone column and correspondingly higher flux of radiation.

For all model cases with $HNO_3 \geq 3$ ppbv, $ClONO_2$ production exceeds HCl production. However, $ClONO_2$ is destroyed at this altitude, mainly by photolysis, with a timescale of 1-3 days during high-latitude spring. In contrast, HCl loss takes place principally through reaction with OH on a much longer timescale (20 - 30 days). Thus the HCl concentration grows at the expense of $ClONO_2$.

To summarize, in the absence of denitrification, the mixing ratio of O_3 determines two regimes for the chlorine reservoir formation at the end of the spring. For an O_3 mixing ratio greater than about 0.5 ppmv, production of $ClONO_2$ following production of NO_X through photolysis of HNO_3 and reaction of HNO_3 with OH dictates that the $ClONO_2$ reservoir will be formed rapidly and the HCl reservoir will grow slowly. As the O_3 mixing ratio falls below 0.5 ppmv, the calculated Cl/ClO ratio increases nonlinearly, and the net production of the HCl reservoir is dominant. For the cases shown here, the Cl/ClO ratio is nearly 30 times greater for the Antarctic case than for the Arctic. A second signal of this condition is that the NO/NO_2 ratio will be larger in the case of lower O_3. The calculated daytime NO/NO_2 ratio is nearly 10 times larger for the southern hemisphere than for the northern.

The UARS data for the northern and southern hemisphere springs illustrate these two different regimes for the photochemical processes. In the southern hemisphere, during mid to late September and early October, ClO is substantially elevated, and ozone drops steadily, as modeled. The cold temperatures allow ClO to remain close to steady, through heterogeneous reaction of $ClONO_2$ with H_2O on NAT particle surfaces or on cold sulfate (these processes are not distinguishable in the model). Once O_3 falls below about 0.5 ppmv. HCl increases rapidly (in the model) at the expense of $ClONO_2$, despite continued production of NO_X from HNO_3 through photolysis and reaction with OH. The rapid growth in the HCl is similar to the growth seen in the HCl column for ground-based observations reported by *Liu et al.* [1992]. The sunset NO concentrations seen by HALOE also increase steadily throughout October; the ratio of NO/NO_2 is significantly higher in the southern hemisphere than in the northern hemisphere.

In the northern hemisphere, during mid to late February and early March, ClO is only slightly elevated. The high values of $ClONO_2$ compared with the southern hemisphere indicate that formation of the $ClONO_2$ reservoir following production of NO_X from HNO_3 due to photolysis and reaction with OH has already taken place. In this case the Cl/ClO ratio has been limited because the O_3 concentration remained high. The reaction of NO with O_3 will be rapid (i.e., the formation of NO_2 will be rapid), guaranteeing that the ratio NO/NO_2 (equation (3)) will be smaller in this case than in the southern hemisphere. This limits the formation of Cl by reaction of ClO + NO. The rate of the reaction of Cl with O_3 to reform ClO is directly proportional to O_3. These both act to produce a smaller value for the ratio Cl/ClO (equation (2)) for the northern hemisphere. HCl growth is seen by HALOE, as the HCl loss timescale is again much longer than that for $ClONO_2$. However, the rate of growth for HCl is much smaller in the northern hemisphere throughout March, in keeping with the lower ratios of Cl/ClO and NO/NO_2 as calculated by the model, in spite of the continued production of NO_X from HNO_3 and the already high values of $ClONO_2$. As expected, the HALOE observations of NO and NO_2 reflect the different balance between NO and NO_2 in the two regimes.

Conclusions

The UARS observations reveal an interhemispheric difference in springtime formation of the chlorine reservoirs within the Arctic vortex and the Antarctic collar region. The O_3 concentration is much lower, and the HCl increase is much more rapid in the southern hemisphere than in the northern hemisphere. The ratio NO/NO_2 is also observed to be larger in the southern hemisphere. These observations confirm the model calculations of *Prather and Jaffe* [1990]. The observed HCl increase is consistent with a calculated Cl/ClO ratio which is larger in the southern hemisphere as a result of low O_3. Low O_3 reduces the rate at which the reaction Cl + O_3 produces ClO and also increases the rate at which ClO + NO produces Cl by increasing the NO/NO_2 ratio.

Finally, sustained cold temperatures lead to substantial O_3 loss in the collar region of the Antarctic vortex by maintaining a low ratio for NO_X/NO_y. There are two ways to maintain a low value for this ratio: (1) PSC formation, which condenses HNO_3 and prevents NO_X production through photolysis and reaction of HNO_3 with OH, and (2) continued production of HNO_3 and loss of NO_X as a result of heterogeneous reactions on sulfate aerosols. Thus O_3 loss can take place even though temperatures cold enough to produce permanent dehydration and denitrification are not observed and sufficient production of NO_X from HNO_3 occurs to sequester some of the chlorine in the $ClONO_2$ reservoir. This suggests that a northern hemisphere winter with sustained cold temperatures could lead to substantially more O_3 loss than has been observed thus far.

Acknowledgments. The research described in the paper was supported by the EOS Interdisciplinary Science Program and by the NASA Research and Applications Program. Computer resources and funding were provided by the EOS Project.

References

Anderson, D. E., Jr., and S. A. Lloyd, Polar Twilight UV-visible radiation field: Perturbations due to multiple scattering, ozone depletion, stratospheric clouds, and surface albedo, *J. Geophys. Res., 95*, 7429-7434, 1990.

Anderson, J. G., W. B. Brune, S. A. Lloyd, D. W. Toohey, S. P. Sander, W. L. Starr, M. Loewenstein, and J. R. Podolske, Kinetics of O_3 destruction by ClO and BrO within the Antarctic vortex: An analysis based upon in situ ER-2 data,*J. Geophys. Res., 94*, 11,480-11,520, 1989.

Barath, F. T., et al., The Upper Atmosphere Research Satellite Microwave Limb Sounder Instrument, *J. Geophys. Res., 98*, 10,751-10,762, 1993.

Burkholder, J. B., R. K. Talukdar, A. R. Ravishankara, and S. Solomon, Temperature dependence of the HNO_3 UV absorption cross sections, *J. Geophys. Res., 98*, 22,937-22,948, 1993.

DeMore, W. B., S. P. Sander, D. M. Golden, R. F. Hampson, M. J. Kurylo, C. J. Howard, A. R. Ravishankara, C. E. Kolb, and M. J. Molina, Chemical kinetics and photochemical data for use in stratospheric modeling, *JPL Pub. 92-20*, 1992.

de Zafra, R. L., M. Jaramillo, J. Barrett, L. K. Emmons, P. M. Solomon, and A. Parrish, New observations of a large concentration of ClO in the springtime lower stratosphere over Antarctica and its implications for ozone-depleting chemistry, *J. Geophys. Res., 94*, 11,423-11,428, 1989.

Fahey, D. W., K. K. Kelly, S. R. Kawa, A. F. Tuck, M. Loewenstein, K. R. Chan, and L. E. Heidt, Observations of denitrification and dehydration in the winter polar stratospheres, *Nature, 344*, 321-325, 1990.

Lait, L. R., An alternative form for potential vorticity, *J. Atmos. Sci., 51*, 1754-1759, 1994.

Liu, X., R. D. Blatherwick, F. J. Murcray, J. G. Keys, and S. Solomon, Measurements and model calculations of HCl column amounts and related parameters over McMurdo during the austral spring in 1989, *J. Geophys. Res., 97*, 20,795-20,804, 1992.

Mankin, W. G., M. T. Coffey, A. Goldman, M. R. Schoeberl, L. R Lait, and P. A. Newman, Airborne measurements of stratospheric constituents over the Arctic in the winter of 1989, *Geophys. Res. Lett., 27*, 473-476, 1990.

Manney G., et al., Chemical depletion of ozone in the Arctic lower stratosphere during winter 1992-93, *Nature, 370*, 429-434, 1994.

McCormick, M. P., J. M Zawodny, R. E. Veiga, and J. C. Larson, An overview of SAGE I and II ozone measurements, *Planet. Space Sci., 37*, 1567-1586, 1989.

Molina, L. T., and M. J. Molina, Production of Cl_2O_2 from the self-reaction of the ClO radical, *J. Phys. Chem., 91*, 433-436, 1987.

Prather, M. P. and A. H. Jaffe, Global impact of the antarctic ozone hole: chemical propagation, *J. Geophys. Res., 95*, 3473-3492, 1990.

Randel, W., Global atmospheric circulation statistics, 1000-1 mb, Tech. Note *NCAR/TN-366+STR*, Natl. Cent. For Atmos. Res., Boulder, Colo., 1992.

Roche, A. E., J. B. Kumer, J. L. Mergenthaler, CLAES observations of $ClONO_2$ and HNO_3 in the Antarctic stratosphere, between June 15 and September 17, 1992, *Geophys. Res. Lett., 20*, 1223-1226, 1993a.

Roche, A. E., J. B. Kumer, J. L. Mergenthaler, G. A. Ely, W. G. Uplinger, J. F. Potter, T. C. James, and L. W. Sterritt, The Cryogenic Limb Array Etalon Spectrometer (CLAES) on UARS: Experiment description and performance, *J. Geophys. Res., 98*, 10,763-10,776, 1993b.

Russell, J. M., L. L. Gordley, J. H. Park, S. R. Drayson, W. D. Hesketh, R. J. Cicerone, A. F. Tuck, J. E. Frederick, J. E. Harries, and P. J. Crutzen, The Halogen Occultation Experiment, *J. Geophys. Res., 98*, 10,777-10,797, 1993.

Schoeberl, M. R., and L. R. Lait, Conservative coordinate transformations for atmospheric measurements, in *The Use of EOS for Studies of Atmospheric Physics*, edited by G. Visconti and J. Gille, pp. 419-430, North-Holland, New York, 1992.

Schoeberl, M. R., et al., Reconstruction of the constituent distribution and trends in the Antarctic polar vortex from ER-2 flight observations, *J. Geophys. Res., 94*, 16,815-16,845, 1989.

Schoeberl, M. R., et al., The evolution of ClO and NO along air parcel trajectories, *Geophys. Res. Lett., 20*, 2511-2514, 1993.

Schoeberl, M. R., M. Luo, and J. E. Rosenfield, An analysis of the Antarctic Halogen Occultation Experiment trace gas observations, *J. Geophys. Res., 100*, 5159-5172, 1995.

Schumacher, N. J., Upper air temperatures over an Antarctic station, *Tellus, 7*, 87-95, 1955.

Solomon, S., Progress towards a quantitative understanding of Antarctic ozone depletion, *Nature, 347*, 347-354, 1990.

Solomon, S., R. R. Garcia, F. S. Rowland, and D. J. Wuebbles, On the depletion of Antarctic ozone, *Nature, 321*, 755-757, 1986.

Tolbert, M. A., M. J. Rossi, and D. M. Golden, Heterogeneous interactions of $ClONO_2$, HCl and HNO_3 with sulfuric acid surfaces at stratospheric temperatures, *Geophys. Res. Lett., 15*, 847-850, 1988.

Toohey D. W., L. M. Avallone, L. R. Lait, P. A. Newman, M. R. Schoeberl, D. W. Fahey, E. L. Woodbridge, and J. G. Anderson, The seasonal evolution of reactive chlorine in the northern hemisphere stratosphere, *Science, 261*, 1134-1136, 1993.

Waters, J. W., L. Froidevaux, W. G. Read, G. L. Manney, L. S. Elson, D. A. Flower, R. F. Jarnot, and R. S. Harwood, Stratospheric ClO and ozone from the Microwave

Limb Sounder on the Upper Atmosphere Research Satellite, *Nature, 362*, 597-602, 1993.

World Meteorological Organization (WMO), Scientific assessment of ozone depletion: 1991, *Rep. 25*, Global Ozone Res. and Monit. Proj., World Meteorol. Organ., Geneva, 1992.

A. R. Douglass, M. R. Schoeberl, and R. S. Stolarski, Atmospheric Chemistry and Dynamics Branch, NASA Goddard Space Flight Center, Greenbelt, MD 20771. (e-mail douglass@persephone.gsfc.nasa.gov)

S. T. Massie, National Center for Atmospheric Research, P. O. Box 3000, Boulder, CO 80307.

A. E. Roche, Lockheed Palo Alto Research Laboratory, 3251 Hanover Street, Palo Alto, CA 94303.

J. M. Russell III, NASA Langley Research Center, Hampton, VA 23681.

J. W. Waters, Jet Propulsion Laboratory, 4800 Oak Grove Drive, Pasadena, CA 91109-8099.

(Received September 13, 1994; revised December 19, 1994; accepted February 20, 1995.)